



# The effect of asphalt emulsion on the properties of fly ash based geopolymers

Natcha PROMMITYAT<sup>1</sup>, Chiravoot PECHYEN<sup>1</sup>, Pitak LAORATANAKUL<sup>2</sup>, and Benya CHERDHIRUNKORN<sup>1,3,\*</sup>

<sup>1</sup> Materials Innovation and Technology Program, Faculty of Science and Technology, Thammasat University, Pathumthani, 12120, Thailand

<sup>2</sup> National Metal and Materials Technology Center, National Science and Technology Development Agency, Pathumthani, 12120, Thailand

<sup>3</sup> Research Unit in Sustainable Materials and Circular Economy, Thammasat University, Patumthani, 12120, Thailand

\*Corresponding author e-mail: benya@tu.ac.th

## Received date:

14 October 2024

## Revised date:

15 January 2025

## Accepted date:

6 March 2025

## Keywords:

Fly ash;  
Bagasse ash;  
Geopolymer;  
Asphalt emulsion;  
Compressive strength

## Abstract

This research aimed to study the effect of asphalt emulsion (AE) on the properties of fly ash based geopolymers. Solid waste materials used for the production of geopolymer were coal fly ash (FA) 70 wt% and bagasse ash (BA) 30 wt%. Alkaline solution used for the geopolymerization reaction was the mixture of 10 M NaOH and Na<sub>2</sub>SiO<sub>3</sub> with the ratio of 1:2. The liquid and solid (L/S) ratios of 0.6, 0.7 and 0.8 were prepared. The AE of 1 wt%, 3 wt% and 5 wt% were added into the raw materials mixtures. Then, the mixed slurry was casted into a mold for the further tests. The setting time was determined using VICAT. After ageing of 7 day, 14 day, and 28 day, the compressive strength and modulus of rupture (MOR) samples were measured. The results of the study revealed that the sample with the L/S ratio of 0.7 had the best mechanical properties. The additional of AE up to 3 wt% led to an improvement of mechanical properties where the 1 wt% of AE gave the highest compressive strength, Young's modulus and MOR. Bulk density and %water absorption, were determined. Phase structures, chemical structures and microstructures were observed using XRD, FTIR and SEM techniques, respectively.

## 1. Introduction

The industrial and agricultural wastes have been a huge environmental issue around the world. They normally need proper elimination methods which could be costly. The alternative and creative methods for utilizing these wastes should be paid attention to. The enormous research works have been carried out to find the way to utilize these solid wastes. The wastes such as coal fly ash, aluminium dross, sewage sludge, blast furnace slag and sugar cane bagasse ash, are mostly composed of several oxides such as SiO<sub>2</sub>, Al<sub>2</sub>O<sub>3</sub> and CaO, providing the suitable aluminosilicate source that can be used in many applications. One of the attractive applications of these solid wastes is being used as raw materials for geopolymer production. Geopolymers have been interested by many researchers as a cement replacement material. Since the cement production emits huge amount of carbon dioxide directly to the atmosphere causing global warming and climate change, the sustainable alternatives such as geopolymers have been interested [1]. Geopolymer is an inorganic polymer with an amorphous structure made of sialate (silico-oxo-aluminate) chained structures, so called polysialate [2]. It can be produced by the geopolymerization reaction of pozzolanic materials (silica and alumina containing materials) and alkaline solution, such as sodium hydroxide solution and sodium silicate solution [3-5]. Thus, many solid waste materials can be used as the aluminosilicate sources for the geopolymer production and enhance the mechanical and physical properties of geopolymers.

In Mae Moh, Lampang, Thailand, the coal power plant are run for electricity generation [6]. About 40,000 tons of lignite are used per day. Coal combustion takes place at elevated temperature and

produce about 10,000 tons of lignite ash per day, of which about 6,000 tons are small particles, so called "fly ash". Coal fly ash is not a toxic waste according to standard of the Pollution Control Department, Thailand. As it can be used in many applications, the utilization of fly ash is value added and encouraged by the Electricity Generating Authority of Thailand (EGAT). Fly ash contains high amount of silica, alumina, iron oxide and calcium oxide, so it can be used in the cement production. In addition, it was reported by Tao Bai, et al. that fly ash could be used as a raw material for geopolymer mortar which was used as a grouting material in porous asphalt concrete [7]. The results showed that the high liquid/solid ratio of the geopolymer mixture lowered the strength of the material.

In Thailand, there are other wastes that could be good sources of silica such as sugarcane bagasse ash (BA), rice husk ash and other biomass ashes, which are the by-products from the bio mass power plants. Sugarcane is one of the major economic crops for sugar industry in Thailand. Sugarcane bagasse (the by-product from Sugar milling industry) can be used as a fuel source for sugar mills themselves or for the bio mass power plant. BA is a residue waste from the burning process. Due to its high silica content, it can also be used as a pozzolanic material for concrete production [8]. P. Chindaprasirt *et al.* reported that the use of sugarcane bagasse ash in the production of pavement concrete gave rise to the higher compressive strength [9]. Due to the high silica content, BA could also be used as a raw material for geopolymer.

In general, geopolymer has high strength but it is quite rigid and brittle. The use of high elasticity material such as asphalt emulsion incorporating in the geopolymer mixture could offer the higher flexural

strength. The asphalt emulsion consists of 3 major components which are asphalt, water and emulsifier. These three components are introduced into a colloid mill, where the asphalt is sheared into small droplets and kept in a stable suspension by the emulsifier.

The asphalt emulsion can be used without additional heat. The water gradually evaporates from the asphalt emulsion leaving the asphalt film sealing the applied surface [10]. Thus, the asphalt emulsion is very convenient for the application of road surface maintenance as it can be used at the room temperature and improves the water resistance and surface adhesion. There are many studies that have been conducted on asphalt emulsion modified concrete. Recently, the use of asphalt emulsion in concrete work was reported by Hongfei Zhang *et al.* [11]. The asphalt emulsion of 0, 5, 10, 15 and 20 wt% modified concrete were prepared and tested. The 5 wt% of asphalt emulsion modified concrete had the highest compressive strength. In addition, the 10 wt% of asphalt emulsion modified concrete had the better sulphate corrosion resistance and chloride penetration resistance. H. A. Umar *et al.* reported that AE could improve durability of concrete by reducing permeability through a pore-filling effect and enhance damping performance, with a 30.6% increase in damping ratio at 20% AE. However, AE reduces compressive and tensile strength while slightly increasing flexural strength [12]. Only few researchers studied on the asphalt emulsion modified geopolymer materials using geopolymer as the main ingredient. Since the asphalt emulsion contains water, so it is not as strong as asphalt that requires heat for melting during road work. Most of the research works are on the addition of geopolymers to improve the mechanical properties of asphalt emulsion, but there are only few works used asphalt emulsion to modify geopolymers. Yang Gao *et al.* has reported that the addition of 10 wt%, 20 wt%, and 30 wt% of geopolymer mixture into the asphalt emulsion resulted in the faster setting time than the cement mixed asphalt emulsion [13]. This result showed that the interaction between geopolymer and asphalt emulsion was stronger than between cement and asphalt emulsion. Y. Pang *et al.* [14] studied the rheological and mechanical properties of asphalt emulsion modified metakaolin based geopolymer. The results showed that the flexural strength could be improved by the additional of asphalt emulsion up to 8 wt%. The fluidity of geopolymer increased slightly by adding asphalt emulsion.

This research work aims to study the effect of asphalt emulsion on the properties of fly ash and bagasse ash based geopolymers. The mechanical properties were obtained and compared to the Thai industrial standard (TIS 213-2520) [15]. The phase structure, chemical structure and microstructure were investigated using XRD, FTIR and SEM techniques, respectively.

## 2. Experimental

### 2.1 Materials

#### 2.1.1 Solid raw materials

In this work, the solid raw materials used in the fabrication of geopolymers were coal fly ash (FA) from Mae Moh power plant (Lampang, Thailand) and sugarcane bagasse ash (BA) from Biomass power plant (Mitr phol bio power Supanburee, Thailand). The chemical compositions of FA and BA were obtained by X-ray fluorescence

(XRF) as shown in Table 1. The main compositions of FA are SiO<sub>2</sub> (26.75%), CaO (21.59%), Al<sub>2</sub>O<sub>3</sub> (15.20%) and Fe<sub>2</sub>O<sub>3</sub> (14.45%). BA contains quite high SiO<sub>2</sub> (57.69%) and CaO (11.86%). The X-ray diffraction (XRD) was used to identify the phase structures of FA and BA as shown in Figure 1-2. The XRD patterns of FA and BA reveal that the main phases of FA are quartz (SiO<sub>2</sub>, JCPDS No. 46-1045), hydrated lime (Ca(OH)<sub>2</sub>, JCPDS No. 72-0156), hematite (Fe<sub>2</sub>O<sub>3</sub>, JCPDS No. 01-1030) and mullite (3Al<sub>2</sub>O<sub>3</sub>·2SiO<sub>2</sub>, JCPDS No. 15-0776), whereas the major phases of BA are quartz (SiO<sub>2</sub>, JCPDS No. 46-1045) and calcite (CaCO<sub>3</sub>, JCPDS No. 89-5969).

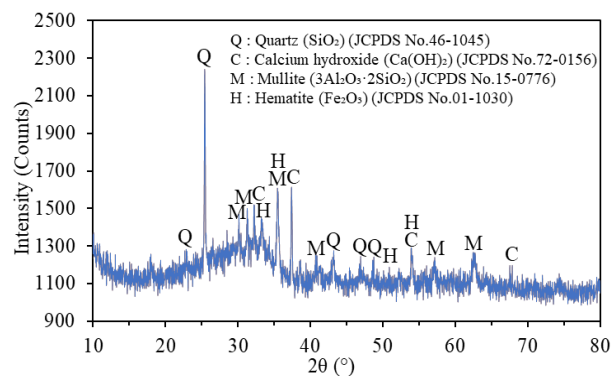


Figure 1. XRD pattern of fly ash.

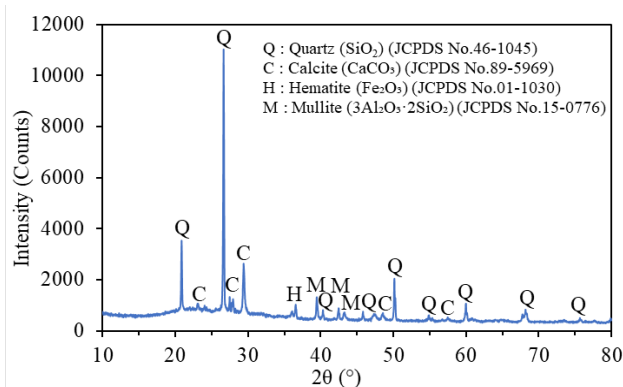


Figure 2. XRD pattern of bagasse ash.

Table 1. Chemical composition expressed in oxides (wt%) of the fly ash and bagasse ash determined by XRF technique.

Composition	Fly ash [wt%]	Bagasse ash [wt%]
SiO <sub>2</sub>	26.75	57.69
CaO	21.59	11.86
Al <sub>2</sub> O <sub>3</sub>	15.20	3.57
Fe <sub>2</sub> O <sub>3</sub>	14.45	2.26
SO <sub>3</sub>	6.01	0.82
MgO	2.09	2.86
K <sub>2</sub> O	1.91	3.63
Na <sub>2</sub> O	1.73	0.25
P <sub>2</sub> O <sub>5</sub>	0.31	2.19
BaO	0.19	0.11
Mn <sub>2</sub> O <sub>3</sub>	0.14	0.23
SrO	0.13	-
TiO <sub>2</sub>	-	0.22
Total	90.50	85.69
Loss on ignition	9.50	14.31

### 2.1.2 Alkali-activating solution

The alkaline solution used for the geopolymerization reaction was a mixture of sodium hydroxide (10 M NaOH) and sodium silicate ( $\text{Na}_2\text{SiO}_3$ ). From preliminary experiments, it was found that the appropriate ratio of NaOH: $\text{Na}_2\text{SiO}_3$  was 1:2 by weight which gave the good flowability of the mixtures for the casting process. After mixing, the mixed NaOH and  $\text{Na}_2\text{SiO}_3$  solution was left at room temperature in a sealed container for 24 h prior mixing with the solid raw materials.

### 2.1.3 Asphalt emulsion (AE)

Asphalt emulsion (Cationic slow setting, CSS-1H type) from Asian Asphalt company limited (Chiang Mai, Thailand) was used as an additive for modifying the geopolymer. In this study, the AE is a water-based asphalt that used water and emulsion without other solvents. The AE is slowly harder after exposing to the air.

## 2.2 Sample preparation of asphalt emulsion modified geopolymers

The preparation method for asphalt emulsion modified geopolymer was shown in Figure 3. The solid raw materials of FA and BA were weighted and mixed according to the FA/BA ratios of 60:40, 70:30 and 80:20 by weight, and were then mixed together with the alkaline solution. Liquid to solid (L/S) ratios were 0.6, 0.7 and 0.80 by weight. The mixtures were casted into a silicone mold (25 mm × 25 mm × 25 mm) for the setting time test (VICAT) and compressive test. The condition with suitable setting time (enough time for casting process) and optimum compressive strength was chosen for the further study. The effects of AE on the properties of geopolymer were studied. The 70 wt% FA and 30 wt% BA powders were mixed with the alkaline solution (L/S ratio of 0.7). Then, the asphalt emulsion of 1 wt%, 3 wt%, and 5 wt% were added into the geopolymer mixtures immediately. After stirring for 3 min, the well mixed slurry was casted into a silicone mold with the size of 25 mm × 25 mm × 25 mm for compressive test and 25 mm × 25 mm × 140 mm for MOR test. The mixtures were left to set at the room temperature. The set of samples were cured at room temperature for 7 day, 14 day, and 28 day, and were then used for the further characterizations (bulk density, water absorption, XRD, FTIR, and SEM) in order to find the best condition to produce AE modified geopolymers with high compressive strength and high MOR.

### 2.3 Sample characterization

The physical properties; bulk density and % water absorption of both FA and BA based (non-AE modified) geopolymers and AE modified geopolymers were determined according to the formula (1-2).

$$\text{Bulk density} = \frac{M}{V} \quad (1)$$

where  $M$  is the weight of sample (g)  
 $V$  is the volume of sample ( $\text{cm}^3$ )

$$\text{Water absorption (\%)} = \left( \frac{W_w - W_d}{W_d} \right) \times 100 \quad (2)$$

where  $W_w$  is the wet weight of sample (g)  
 $W_d$  is the dry weight of sample (g)

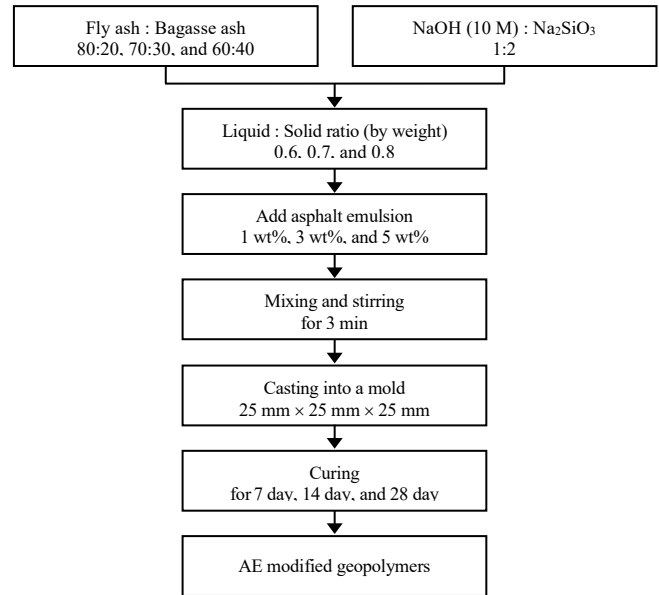


Figure 3. Production process of asphalt emulsion modified geopolymers.

The mechanical properties, including compressive strength, Young's modulus ( $E$ ) and modulus of rupture (MOR) of the samples cured at 7 day, 14 day, and 28 day were obtained using Universal Testing Machine, Tinius Olsen H50KT with the loading speed of  $5 \text{ mm} \cdot \text{min}^{-1}$ . The compressive strength of the samples with the size of  $2.5 \text{ mm} \times 2.5 \text{ mm} \times 2.5 \text{ mm}$  was calculated via the formula (3).

$$\text{Compressive strength} = \frac{F}{A} \quad (3)$$

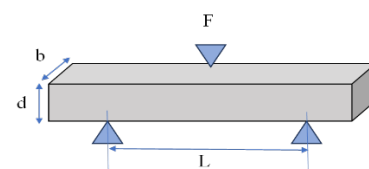
where  $F$  is applied compressive force (N)  
 $A$  is original cross-sectional area of sample ( $\text{m}^2$ )

Young's modulus ( $E$ ) is a measure of the stiffness of the sample, determining from the linear elastic region of the stress-strain curve, defined as (4).

$$E = \frac{\sigma}{\epsilon} \quad (4)$$

where  $\sigma$  is stress (Pa)  
 $\epsilon$  is strain

Modulus of rupture (MOR) of the samples with the size of  $25 \text{ mm} \times 25 \text{ mm} \times 140 \text{ mm}$  was determined via three point bending method and calculated via the formula (5). The supporting span length ( $L$ ) for this measurement was fixed at 100 mm.



$$\text{MOR} = \frac{3FL}{2bd^2} \quad (5)$$

where  $F$  is applied force (N)  
 $L$  is supporting span length (m)  
 $b$  is the width of sample (m)  
 $d$  is thickness of sample (m)

Phase structures of non-AE and 1% AE modified geopolymer samples cured for 28 day were analyzed by the X-ray diffractometer (Bruker/D2 PHASER) from  $2\theta$  of  $5^\circ$  to  $80^\circ$  with the time per step of 0.2 s. The Fourier Transform Infrared spectrometer (SHIMADZU IR Spirit, QATR-S) was employed to observe the chemical structure of the samples after curing for 28 day (non-AE, 1 wt%, 3 wt%, and 5 wt% AE modified geopolymers). All FTIR spectra were recorded between the wavenumber of  $400\text{ cm}^{-1}$  and  $4000\text{ cm}^{-1}$ . In addition, the microstructural features of non-AE, 1 wt%, 3 wt%, and 5 wt% AE modified geopolymers were investigated using Scanning Electron Microscopy (JEOL JSM-7800F).

### 3. Results and discussion

#### 3.1 The effect of FA:BA contents and L/S ratios on the setting time and compressive strength of geopolymers

Figure 4 shows the setting time of geopolymer samples with FA:BA contents of 60:40, 70:30 and 80:20 and L/S ratios of 0.6, 0.7, 0.8. The increase of L/S results in the faster setting time of the geopolymers. The sample with the FA:BA content of 60:40 and L/S ratio of 0.6 was unable to measure its setting time and compressive strength as the strong reaction occurred and the mixture set too fast (unable to cast into a mold). The results shows that the setting time increases with the higher L/S ratios. The samples with FA:BA content of 70:30 and 60:40 and L/S ratio of 0.8 took the longest setting time (about 23 min). These results agree with the previous research works of N. Toobpeng *et al.* [16] and T. Bualuang *et al.* [17]

The compressive strengths of the samples with FA:BA contents of 60:40, 70:30 and 80:20 by weight and L/S ratios of 0.6, 0.7, 0.8 by weight are shown in Figure 5. It was found that the sample with FA:BA content of 70:30 and L/S ratio of 0.6 had the highest compressive strength of 9.07 MPa. However, the setting rate of the sample with L/S ratio of 0.6 was only 13 min, so its castability was poor (the mixture become hard before finishing the casting process). For the samples with FA:BA content of 60:40 both with L/S ratios of 0.7 and 0.8, their compressive strength was slightly higher than other samples, but they set before finishing the casting process, thus it was difficult for casting process. Consequently, the FA:BA content of 70:30 and the L/S ratios of 0.7 and 0.8 were chosen for the further studies of the AE modified geopolymers because the strength of these specimens was higher than the specimens with the FA:BA content of 80:20 and L/S ratios of 0.7 and 0.8. In addition, they had a suitable setting time of 19 min which was enough time for casting process.

#### 3.2 The effect of AE on the properties of FA and BA based geopolymers

##### 3.2.1 Setting time

The chosen composition of FA and BA based geopolymers used in this study were FA:BA content of 70:30 with L/S ratios of 0.7 and 0.8 by weight. The 1 wt%, 3 wt% and 5 wt% of AE added into the geopolymer mixtures affected the setting time of geopolymers as shown in Figure 6. The addition of 1 wt% of AE slightly reduced the setting time as the addition of AE, which consists of water, caused

the higher water content in the mixture. The further increase of AE contents (3 wt% and 5 wt%) markedly slowed down the setting time of the geopolymer samples. This higher amount of AE could cause the separation of the particles of raw materials, resulting in a slower reaction. The 5 wt% AE caused the slowest setting time of 40 min for sample with L:S = 0.7 and 60 min for the sample with L:S = 0.8.

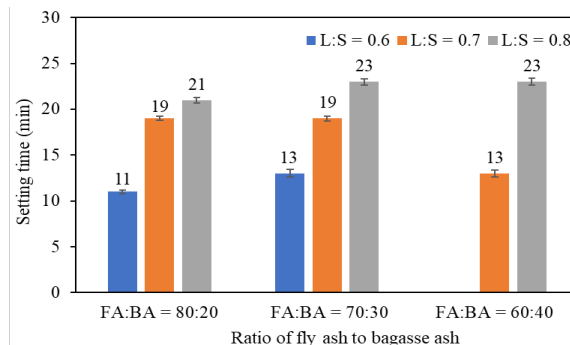


Figure 4. Setting time of geopolymer samples.

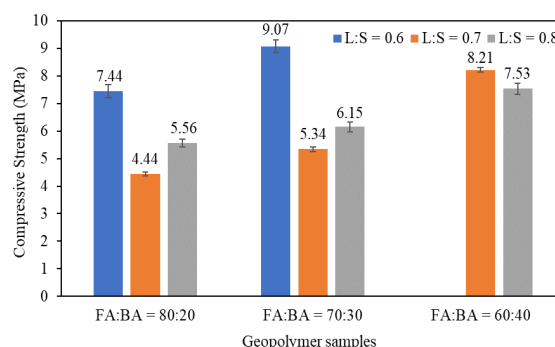


Figure 5. Compressive strength of geopolymer.

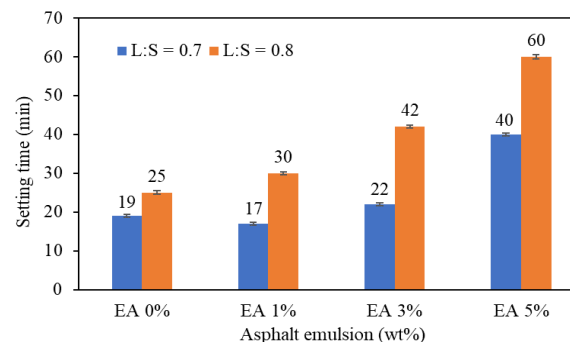


Figure 6. The setting time of AE modified geopolymers.

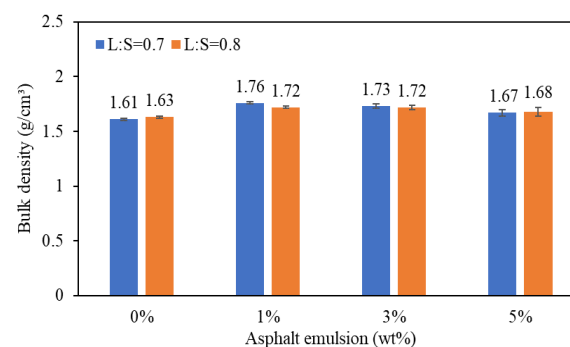


Figure 7. Bulk density of AE modified geopolymers.

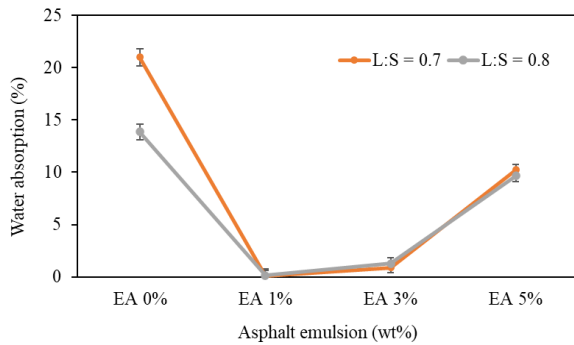


Figure 8. Water absorption (%) of AE modified geopolymers.

### 3.2.2 Bulk density and water absorption

The bulk density and % water absorption of the non-AE and AE modified geopolymer samples are shown in Figure 7-8. The L/S ratios and the addition of AE did not affect much on the bulk density. All the samples had the density between  $1.63 \text{ g}\cdot\text{cm}^{-1}$  to  $1.76 \text{ g}\cdot\text{cm}^{-1}$ . For the non-AE modified geopolymer samples, the water absorption of sample with L/S of 0.8 was slightly lower than that of the one with L/S of 0.7 by weight. The addition of AE up to 1 wt% caused the reduction of water absorption dramatically. The 3 wt% of AE resulted in the low water absorption as well. However, the further increase of AE up to 5 wt% gave rises to the higher water absorption. The results indicated that the small amount of AE (1 wt% and 3 wt%) could be well penetrated though the pores in the geo-polymer samples resulted in the lower porosity and lower water absorption

### 3.2.3 Mechanical properties

Compressive strength and modulus of rupture (MOR) of the geopolymer samples both with and without AE cured at room temperature for 7 day, 14 day, and 28 day were determined using a Universal testing machine. The results shown in Figure 9 indicated that the longer curing time give rise to the higher strength. In addition, it was found that AE could increase the compressive strength and MOR of geopolymer samples as the AE could penetrated through the pores in the sample giving the denser and less porosity samples as shown in previous results (Figure 7-8). The highest strength (14.38 MPa) was obtained in the 1% AE modified geopolymer sample whereas the further increase of AE (3% and 5%) shows the reduction of strength. This suggests that the limited amount of AE could be incorporated into the mixture of geopolymer. The exceed amount of AE could cover around the particle of raw materials during the reaction and delay the reaction, and thus lower strength was obtained in these samples. This agrees with the work reported by Thanon Bualuang *et al.* [17] In addition, Figure 10 shows that the Young's modulus (E) of the samples (L/S = 0.7) decreases as an increase of AE content indicating that AE could increase the strain and reduce the stiffness of the samples.

From the MOR measurements (Figure 11) of the asphalt emulsion modified geopolymers cured for 7 day, 14 day, and 28 day, the addition of asphalt emulsion results in a decrease of MOR. All the samples with L/S ratio of 0.7 show the higher MOR comparing to the samples with L/S ratio of 0.8. The longer curing time yielded the higher MOR where the non-asphalt emulsion modified geopolymer gave the highest MOR of 2.48 MPa.

### 3.2.4 X-ray diffraction

The XRD patterns shown in Figure 12 reveals the phase structures of the non-AE and 1 wt% AE modified geopolymers. The broad peak at  $2\theta$  of  $20^\circ$  to  $35^\circ$  indicates the formation of an amorphous structure during the geopolymerization reaction. This confirms the geopolymerization reaction of raw materials. However, there are some crystalline phases that belong to the unreacted raw materials presented in the XRD patterns of both samples, for example, quartz and calcite phases.

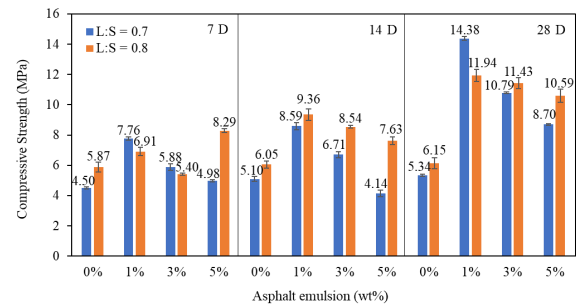


Figure 9. Compressive strength of geopolymer mixed with asphalt emulsion.

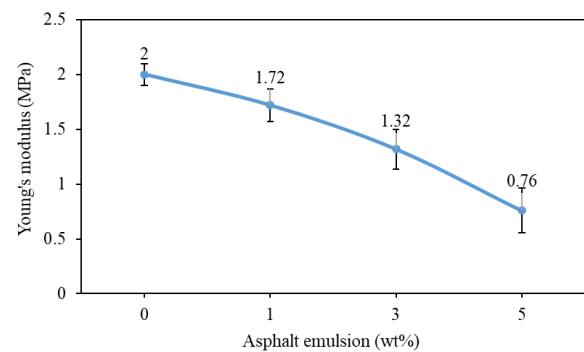


Figure 10. Young's modulus of geopolymer mixed with asphalt emulsion.

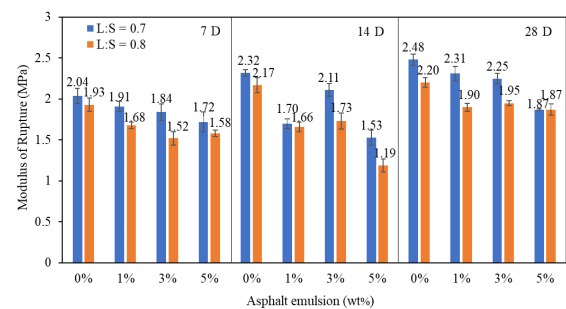


Figure 11. Modulus of rupture of geopolymer mixed with asphalt emulsion.

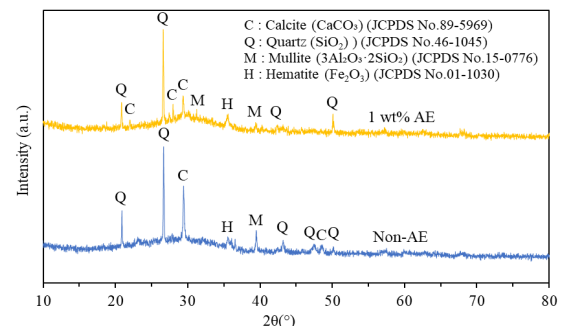
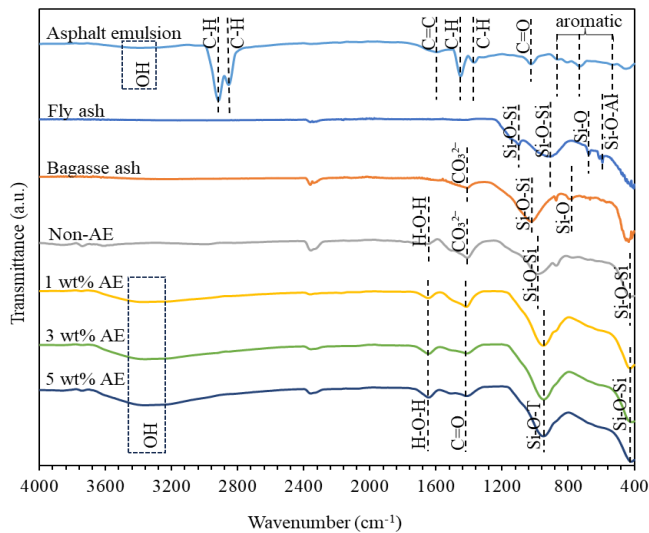
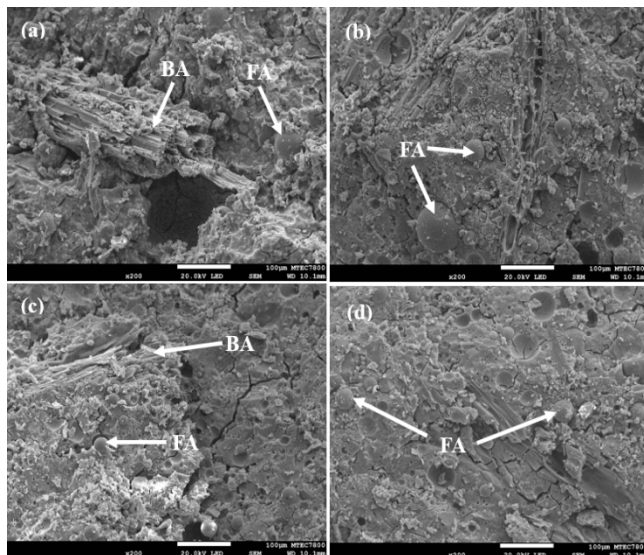


Figure 12. XRD patterns of non-AE and 1 wt% AE geopolymers.





**Figure 13.** FTIR spectra of geopolymer and geopolymer mixed with asphalt 1 wt%, 3 wt%, and 5 wt% compared with raw materials.



**Figure 14.** SEM of non-AE and AE modified geopolymer samples. (a) non-AE, (b) 1 wt% AE, (c) 3 wt% AE, and (d) 5 wt% AE.

### 3.2.5 Fourier transform infrared spectroscopy

Fourier transform infrared (FTIR) spectra of the raw materials and geopolymers with AE and without AE are given in Figure 13. In AE modified geopolymer, transmittance at  $3450\text{ cm}^{-1}$  and  $1650\text{ cm}^{-1}$  can be attributed to (H-O-H) asymmetric stretching due to water and silanol groups. Broad peak centered around  $1020\text{ cm}^{-1}$  is assigned to Si-O-T (T=Si or Al) vibrations in fly ash and geopolymers. Si-O-T bonding vibration provides valuable information about geopolymerization. In solid raw materials, the asymmetric stretching vibration of Si-O-Si of FA and BA appeared at  $1097\text{ cm}^{-1}$  and  $1023\text{ cm}^{-1}$ , respectively. This Si-O-Si band shifted to the lower wave numbers of  $984\text{ cm}^{-1}$  for non-AE modified geopolymer sample indicating the development of amorphous silicon aluminate gels [18]. This new peak formation can be explained on transformation of Si-O-Si bonds of amorphous silica into Si-O-Al bonds of poly sialate. This similar to the work reported by Temujin *et al.* [19] where the Si-O-T peak at  $1100\text{ cm}^{-1}$  in fly ash was disappeared

and a new peak at  $965\text{ cm}^{-1}$  appeared due to geopolymerization. The addition of 1 wt%, 3 wt% and 5 wt% of AE into the geopolymers caused the band shifting to the lower wave number of  $950\text{ cm}^{-1}$ . A shoulder at  $1100\text{ cm}^{-1}$  in geopolymer samples is due to presence of quartz. All geopolymer samples have nearly similar spectra with a minor variation in broadening of peak. Ailar *et al.* [19] used in situ ATR-FTIR for early stages study of geopolymer. Si-O-T transmission peak of fly ash at  $1050\text{ cm}^{-1}$  was found to transform into a new peak at  $960\text{ cm}^{-1}$  due to Si-O-Al bonds formation. In lower silicates the peak position is centred around  $990\text{ cm}^{-1}$  [20].

### 3.2.6 Microstructure

SEM images of the fracture surface of geopolymer samples with 1 wt%, 3 wt%, and 5 wt% AE and without AE are shown in Figure 14. In all samples, there are some remain raw materials, such as, fly ash particles (spherical particles) and bagasse ash (large wooden look particles). There is no obvious segregation phase of asphalt emulsion that added to geopolymer, so the AE could be homogeneously blended into a mixture of the geopolymer. This is consistent with the FTIR results in section 3.6, which did not show any peaks of the asphalt emulsion in the 1 wt%AE modified geopolymer.

## 4. Conclusions

- The appropriate composition of FA and BA based geopolymer is the ratio of FA:BA at 70:30 with the L/S ratio of 0.7. This composition has a setting time of 19 min, allowing enough time to mix all raw materials before casting into a mold. The compressive strength achieved was 5.34 MPa.
- The 1 wt% AE enhanced the compressive strength of the geopolymer sample curing for 28 day, while the non-AE modified geopolymer sample yielded the highest modulus of rupture of 2.48 MPa. The addition of 1 wt% AE in geopolymer also resulted in lowest water absorption of 0.12%. This demonstrates that adding asphalt emulsion to the geopolymer product leads to the raw materials bonding into an amorphous structure, significantly enhancing the strength of the product.

## Acknowledgement

This work was supported by Thammasat University Research unit in Sustainable Materials and Circular Economy. The researchers would like to thank the support of the Electricity Generating Authority of Thailand, Mae Moh Power Plant, and Asian Asphalt Co., Ltd.

## References

- [1] P. D. Nukah, S. J. Abbey, C. A. Booth, and J. Oti, "Development of low carbon concrete and prospective of geopolymer concrete using lightweight coarse aggregate and cement replacement materials," *Construction and Building Materials*, vol. 428, pp. 136295, 2024.
- [2] Z. Moujoud, S. Sair, H. Ait Ousaleh, I. Ayouch, A. El Bouari, and O. Tanane, "Geopolymer composites reinforced with natural

- fibers: A review of recent advances in processing and properties," *Construction and Building Materials*, vol. 388, p. 131666, 2023.
- [3] A. Naghizadeh, L. N. Tchadjie, S. O. Ekolu, and M. Welman-Purchase, "Circular production of recycled binder from fly ash-based geopolymer concrete," *Construction and Building Materials*, vol. 415, p. 135098, 2024.
- [4] V. Vanathi, V. Nagarajan, and P. Jagadesh, "Influence of sugarcane bagasse ash on mechanical properties of geopolymer concrete," *Journal of Building Engineering*, vol. 79, p. 107836, 2023.
- [5] R. Somna, T. Saowapun, K. Somna, and P. Chindapasirt, "Rice husk ash and fly ash geopolymer hollow block based on NaOH activated," *Case Studies in Construction Materials*, vol. 16, p. e01092, 2022.
- [6] S. Ayasanond. "Fly ash concrete." Materialsroom.com. <https://materialsroom.com/2021/06/24/fly-ash-concrete/> [Accessed 20 February 2024].
- [7] T. Bai, Y. Liang, C. Li, X. Jiang, Y. Li, C. Anqi, H. Wang, F. Xu, and C. Peng, "Application and validation of fly ash based geopolymer mortar as grouting material in porous asphalt concrete," *Construction and Building Materials*, vol. 332, p. 127154, 2022.
- [8] S. Rugthaicharoencheep. "Coated with bagasse ash." Thailand Techshow.com. [https://www.thailandtechshow.com/view\\_techno.php?id=190](https://www.thailandtechshow.com/view_techno.php?id=190) [Accessed 20 February 2024].
- [9] P. Chindapasirt, P. Sujumngtokul, and P. Posi, "Durability and mechanical properties of pavement concrete containing bagasse ash," *Materials Today: Proceedings*, vol. 17, pp. 1612-1626, 2019.
- [10] T. Asphalt. "Asphalt Emulsion" Tipcoasphalt.com. <https://www.tipcoasphalt.com/products-services/asphalt-emulsion/> [Accessed 20 February 2024].
- [11] H. Zhang, J. Zhang, Y. Yang, Q. Hu, Y. He, and P. Wei, "Effects of asphalt emulsion on the durability of self-compacting concrete," *Construction and Building Materials*, vol. 292, p. 123322, 2021.
- [12] H. A. Umar, X. Zeng, X. Lan, H. Zhu, Y. Li, and H. Liu, "Evaluation of the influence of asphalt emulsion on the strength, durability, and damping performance of filling layer self-compacting concrete," *Journal of Civil Engineering*, vol. 26, pp. 5082-5095, 2022.
- [13] Y. Gao, Z. Hao, X. Zhang, D. Wang, F. Li, and Z. Zhao, "Interaction, rheological and physicochemical properties of emulsified asphalt binders with direct coal liquefaction residue based geopolymers," *Construction and Building Materials*, vol. 384, p. 131444, 2023.
- [14] Y. Pang, X. Zhu, M. Yang, and J. Yu, "Tailoring rheological–strength–ductility properties of self-cleaning geopolymer composites with asphalt emulsion," *Construction and Building Materials*, vol. 308, p. 124997, 2021.
- [15] C. Academy. "Compressive concrete." cpacademy.com. <https://www.cpacademy.com/E-Books0> [Accessed 20 February 2024].
- [16] N. Toobpeng, P. Thavorniti, and S. Jiemsirilers, "Effect of additives on the setting time and compressive strength of activated high-calcium fly ash-based geopolymers," *Construction and Building Materials*, vol. 417, p. 135035, 2024.
- [17] T. Bualuang, P. Jitsangiam, and T. Tanchaisawat, "Sustainable flexible pavement base stabilization with pozzolanic materials incorporating sodium hydroxide and asphalt emulsion," *Transportation Engineering*, vol. 6, p. 100094, 2021.
- [18] T. Mukhametkaliyev, M. H. Ali, V. Kutugin, O. Savinova, and V. Vereschagin, "Influence of mixing order on the synthesis of geopolymer concrete," *Polymers*, vol. 14, no. 21, 2022.
- [19] J. Temuujin, R. P. Williams, and A. van Riessen, "Effect of mechanical activation of fly ash on the properties of geopolymer cured at ambient temperature," *Journal of Materials Processing Technology*, vol. 209, no. 12, pp. 5276-5280, 2009.
- [20] A. Hajimohammadi, J. L. Provis, and J. S. J. van Deventer, "Time-resolved and spatially-resolved infrared spectroscopic observation of seeded nucleation controlling geopolymer gel formation," *Journal of Colloid and Interface Science*, vol. 357, no. 2, pp. 384-392, 2011.